Molecular Biology of the Cell
Vol. 18, 4387–4396, November 2007

RAB-10 Regulates Glutamate Receptor Recycling in a Cholesterol-dependent Endocytosis Pathway

Doreen R. Glodowski,*† Carlos Chih-Hsiung Chen,‡ Henry Schaefer,*† Barth D. Grant,‡ and Christopher Rongo*†

*The Waksman Institute, †Department of Genetics, and ‡Department of Molecular Biology and Biochemistry, Rutgers University, Piscataway, NJ 08854

Submitted May 23, 2007; Revised August 6, 2007; Accepted August 20, 2007
Monitoring Editor: Tom U. Martin

Regulated endocytosis of α-amino-3-hydroxy-5-methyl-4-isoxazolepropionic acid-type glutamate receptors (AMPARs) is critical for synaptic plasticity. However, the specific combination of clathrin-dependent and -independent mechanisms that mediate AMPAR trafficking in vivo have not been fully characterized. Here, we examine the trafficking of the AMPAR subunit GLR-1 in *Caenorhabditis elegans*. GLR-1 is localized on synaptic membranes, where it regulates reversals of locomotion in a simple behavioral circuit. Animals lacking RAB-10, a small GTPase required for endocytic recycling of intestinal cargo, are similar in phenotype to animals lacking LIN-10, a postsynaptic density 95/disc-large/zona occludens-domain containing protein: GLR-1 accumulates in large accretions and animals display a decreased frequency of reversals. Mutations in *unc-11* (AP180) or *itsn-1* (Intersectin 1), which reduce clathrin-dependent endocytosis, suppress the *lin-10* but not *rab-10* mutant phenotype, suggesting that LIN-10 functions after clathrin-mediated endocytosis. By contrast, cholesterol depletion, which impairs lipid raft formation and clathrin-independent endocytosis, suppresses the *rab-10* but not the *lin-10* phenotype, suggesting that RAB-10 functions after clathrin-independent endocytosis. Animals lacking both genes display additive GLR-1 trafficking defects. We propose that RAB-10 and LIN-10 recycle AMPARs from intracellular endosomal compartments to synapses along distinct pathways, each with distinct sensitivities to cholesterol and the clathrin-mediated endocytosis machinery.

INTRODUCTION

Continuous movement of α-amino-3-hydroxy-5-methyl-4-isoxazolepropionic acid (AMPA)-type glutamate receptors (AMPARs) into and out of synaptic membranes is a key mechanism for the regulation of excitatory synaptic strength. Previous work has shown that insertion of AMPARs into the plasma membrane strengthens synapses and that it is required to convert silent synapses into active synapses (Bredt and Nicoll, 2003; Malenka, 2003; Malinow, 2003; Sheng and Hyoung Lee, 2003; Gerges *et al.*, 2005). Furthermore, it has recently been shown that recycling of AMPARs from internal endosomal compartments back to the plasma membrane is important for long-term potentiation (Park *et al.*, 2004). By contrast, endocytosis of AMPARs at sites adjacent to the postsynaptic density is important for long-term depression (Carroll *et al.*, 2001; Racz *et al.*, 2004). Thus, molecular machinery required for endocytosis, as well as intracellular membrane trafficking processes, ultimately regulates the character of signal transmitted at each synapse.

Multiple endocytosis trafficking pathways have been observed in cells. Clathrin-dependent endocytosis occurs at clathrin-coated pits, where transmembrane protein cargo and adaptor molecules recruit soluble clathrin (Le Roy and Wrana, 2005). Vesicles coated with a clathrin lattice are then pinched off from the membrane. Members of the Rab family of small guanosine triphosphate (GTP)ases mediate the intracellular membrane trafficking of endocytosed vesicles to early endosomes, where they fuse and release their cargo (Clague, 1998; Zerial and McBride, 2001). Such clathrin-dependent endocytosis plays an important role in the regulated removal of AMPARs from the synapse, and it is regulated by the small GTPase Rab5 (Carroll *et al.*, 1999; Man *et al.*, 2000; Wang and Linden, 2000; Burbea *et al.*, 2002; Brown *et al.*, 2005).

Clathrin-independent endocytosis can also occur in cells. Clathrin-independent pathways proceed through cholesterol and sphingolipid-rich microdomains (lipid rafts), and regulate the levels and activity of growth factor signaling molecules (Johannes and Lamaze, 2002; Parton and Richards, 2003; Kirkham and Parton, 2005; Le Roy and Wrana, 2005). It is not clear whether AMPARs are endocytosed by clathrin-independent pathways, although lipid rafts have been observed in dendrites of cultured hippocampal neurons (Hering *et al.*, 2003).

One factor that has been associated with clathrin-independent endocytosis is RAB-10, a broadly expressed Rab that directs protein trafficking in polarized cells of both mammals and *Caenorhabditis elegans* (Babbey *et al.*, 2006; Chen *et al.*, 2006). Work done in the intestinal epithelial cells of *C. elegans* suggests that RAB-10 mediates cargo recycling from early endosomes back to the basolateral membrane (Chen *et al.*, 2006). Mutants for *rab-10* fail to recycle transmembrane cargo, resulting in enlarged early endosomes. Cargo endocytosed by clathrin-independent endocytosis (e.g., the interleukin-2 receptor) are particularly dependent on RAB-10 for recycling. Given the particularly strong requirement for RAB-10 in regulating clathrin-independent cargo, RAB-10 is

This article was published online ahead of print in *MBC in Press* (http://www.molbiolcell.org/cgi/doi/10.1091/mbc.E07–05–0486) on August 29, 2007.

Address correspondence to: Christopher Rongo (rongo@waksman.rutgers.edu).

a possible candidate for a clathrin-independent regulator of AMPAR trafficking.

AMPAR trafficking and localization can be studied in the intact nervous system of the genetically tractable model organism *C. elegans* (Rongo *et al.*, 1998). The *C. elegans* genome contains two AMPAR-type subunits: GLR-1 and GLR-2 (Hart *et al.*, 1995; Maricq *et al.*, 1995; Brockie *et al.*, 2001a). Previously, we showed that fluorescently tagged versions of GLR-1 are functional and that they are localized to postsynaptic regions when expressed in nematodes (Rongo *et al.*, 1998). Furthermore, GLR-1 is required at interneurons that are part of a simple sensory circuit regulating backward movement, both in response to nose-touch stimulus and as part of the foraging behavior of animals. Mutants with depressed GLR-1 synaptic levels are nose-touch defective and rarely reverse direction, whereas mutants with elevated synaptic levels reverse direction with increased frequency (Hart *et al.*, 1995; Maricq *et al.*, 1995; Zheng *et al.*, 1999; Brockie *et al.*, 2001b; Mellem *et al.*, 2002; Schaefer and Rongo, 2006). Therefore, by observing the behavior (e.g., nose-touch response and reversals per minute) of animals with different genetic backgrounds, we can compare signal strength at this circuit, and we can infer the abundance of GLR-1 AMPARs present at the postsynaptic plasma membrane.

Like mammalian AMPARs, GLR-1 synaptic abundance is regulated by clathrin-dependent endocytosis (Burbea *et al.*, 2002). Mutations in *unc-11*, an orthologue of the AP180 clathrin adaptin protein, result in the increased accumulation of GLR-1 at synaptic sites. It is unclear whether clathrin-independent pathways also mediate GLR-1 endocytosis, or whether multiple endocytosis pathways regulate AMPAR trafficking in general. Here, we identify RAB-10 as a regulator of a novel AMPAR endocytosis and trafficking pathway. We show that *rab-10* mutant animals display defects in GLR-1 localization and behavior consistent with an intracellular endosomal accumulation of GLR-1 in neurites. These mutant phenotypes were rescued cell-autonomously by expression of a *rab-10* cDNA. Furthermore, we provide evidence to suggest that RAB-10 functions in a genetic pathway parallel to that of LIN-10, a postsynaptic density 95/disc-large/zona occludens (PDZ)-domain protein of the Mint/X11 family previously shown to be involved in AMPAR trafficking (Rongo *et al.*, 1998; Glodowski *et al.*, 2005). We propose that RAB-10 and LIN-10 are components of two distinct pathways that regulate trafficking of different pools of AMPARs at synapses.

MATERIALS AND METHODS

Genetics and Strains

Standard methods were used to culture *C. elegans*. The following strains were used: N2, *lin-10(e1439)*, *lin-10(n1508)*, *unc-11(e47)*, *rab-10(dx2)*, *rab-10(q373)*, *itsn-1(ok268)*, *odIs22*[$P_{glr\text{-}1}$::*LIN-10::GFP*], *odIs1*[$P_{glr\text{-}1}$::*SNB-1::GFP*], *odIs42*[$P_{glr\text{-}1}$::*RFP::RAB-10*], *nuIs89*[$P_{glr\text{-}1}$::*MUb*], and *nuIs25*[*GLR-1::GFP*].

Transgenes and Germline Transformation

Transgenic strains were isolated after microinjecting various plasmids (5–50 ng/μl) by using *rol-6dm* (a gift from C. Mello, University of Massachusetts Medical School), red fluorescent protein (RFP) (monomeric RFP; a gift from R. Tsien, Stanford University School of Medicine), or *lin-15(+)* (a gift from J. Mendel, Cal Tech) as a marker (Campbell *et al.*, 2002). Plasmids containing the *glr-1* promoter, followed by a gene encoding either RFP::RAB-10 or RFP::RME-1, were introduced into the germline and followed as extrachromosomal arrays. To generate these plasmids, LR Clonase reactions (Gateway Technology; Invitrogen, Carlsbad, CA) were performed using entry clones containing genomic DNA encoding RME-1 or cDNA encoding RAB-10. For these reactions, the destination vector, which contains the *glr-1* promoter upstream of a *ccdB* gene that is flanked by *attR* sites, was generated from the plasmid, pV6 (a gift from V. Maricq, University of Utah), following manufacturer's protocols (Invitrogen). For RFP::RAB-10, stable transgenic lines, including *odIs42*, were obtained by γ-irradiation followed by four generations of backcrossing.

Fluorescence Microscopy

Green fluorescent protein (GFP)- and RFP-tagged fluorescent proteins were visualized in nematodes by mounting larvae on 2% agarose pads with 10 mM levamisole. Fluorescent images were observed using an Axioplan II (Carl Zeiss, Thornwood, NY). A 100× (numerical aperture 1.4) PlanApo objective was used to detect GFP and RFP signal. Imaging was done with an ORCA charge-coupled device camera (Hamamatsu, Bridgewater, NJ) by using IPLab software (Scanalytics, Fairfax, VA). Exposure times were chosen to fill the 12-bit dynamic range without saturation. Maximum intensity projections of z-series stacks were obtained, and out-of-focus light was removed with a constrained iterative deconvolution algorithm. Cluster outlines were automatically calculated for fluorescent signals that were two standard deviations above the unlocalized baseline by using a macro written for IPLabs. Cluster size was measured as the maximum diameter for each outlined cluster. Cluster outline data included both small puncta (e.g., as observed in wild type), as well as long accretions (e.g., as observed in *lin-10* and *rab-10* mutants). Cluster number was calculated by counting the average number of clusters per 10 μm of dendrite length.

Behavioral Assays

Nose-touch sensory responses were assayed as described previously (Hart *et al.*, 1995). Each animal was tested on food for reversal of locomotion after a forward collision with a hair. Each animal was tested 10 times, and 20 or more animals were tested for each genotype. The reversal frequency of individual animals was assayed as described previously, but with some modifications (Zheng *et al.*, 1999). Single young adult hermaphrodites were placed on nematode growth medium plates in the absence of food. The animals were allowed to adjust to the plates for 5 min, and the number of spontaneous reversals for each animal was counted over a 5-min period. Animals in Figure 4F were touched on their posterior every 20 s to induce forward locomotion. Twenty animals were tested for each genotype, and the reported scores reflect the mean number of reversals per minute.

Growth on Cholesterol-depleted Media

For cholesterol-depleted growth of *C. elegans*, both OP50 bacterial media and *C. elegans* plate media were prepared using ether-extracted peptone as described previously (Merris *et al.*, 2003). Gravid animals were placed on plates containing cholesterol-depleted media, and they were allowed to lay eggs overnight. Adult animals were then removed, and the eggs were hatched and raised on cholesterol-depleted media. On reaching adulthood, animals were examined for GLR-1 fluorescence as described above.

RESULTS

RAB-10 Is a Novel Regulator of GLR-1 Trafficking

In the command interneurons of *C. elegans*, postsynaptic localization of a GFP-tagged version of the AMPAR subunit GLR-1 (GLR-1::GFP) has been characterized previously (Rongo *et al.*, 1998). GLR-1::GFP is localized to small, multitudinous, synaptic clusters in the neurites of wild-type animals (Figure 1A). Because RAB-10 is expressed in neurons as well as epithelia (Chen *et al.*, 2006), we tested whether RAB-10 regulates the postsynaptic localization of AMPARs, comparing the localization of GLR-1::GFP in a wild-type background to that in two different *rab-10* loss of function mutant backgrounds. Similar results were observed with both mutant alleles. In *rab-10* mutant animals, we observed an accumulation of GLR-1::GFP in large accretions running along the length of the ventral cord neurite bundle (Figure 1B). The size of these accretions is reminiscent of the intracellular membrane-bound compartments observed in the neurites of the ventral cord (Rolls *et al.*, 2002). The *rab-10* mutant phenotype is similar to the phenotype resulting from mutations in LIN-10 (Figure 1C), a PDZ domain protein of the Mint/X11 family (Borg *et al.*, 1998; Butz *et al.*, 1998; Rongo *et al.*, 1998; Whitfield *et al.*, 1999). LIN-10/Mint/X11 proteins regulate AMPAR trafficking; however, their mechanism of action is unclear (Rongo *et al.*, 1998; Stricker and Huganir, 2003).

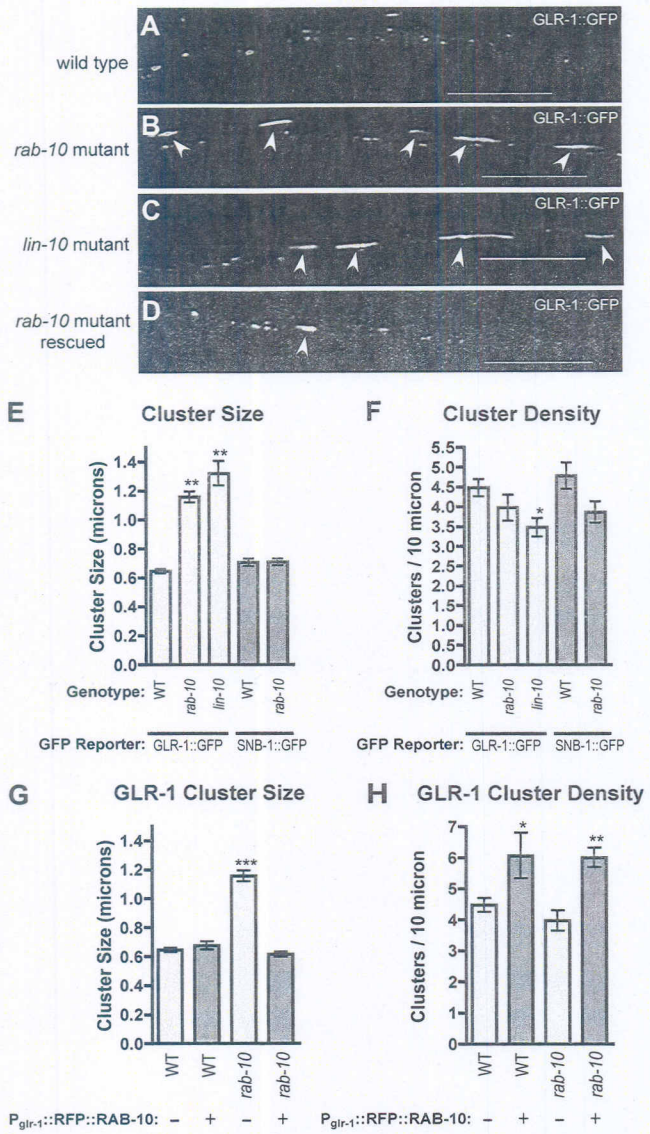

Figure 1. RAB-10 regulates GLR-1 trafficking. GLR-1::GFP fluorescence was observed along ventral cord dendrites of wild-type animals (A), *rab-10* mutants (B), *lin-10* mutants (C), or *rab-10* mutants (D) that express a wild-type *rab-10* cDNA (with RFP fused in frame at N terminus) by using the *glr-1* promoter. The mean size (E) and the mean density (F; number per 10 μm of ventral cord) of fluorescent puncta are plotted for adult nematodes of the given genotype and for the given fluorescent reporter (either GLR-1::GFP, light gray bars, or SNB-1::GFP, dark gray bars). The mean size (G) and density (H) of GLR-1 clusters are plotted for either wild type or rab-10 mutant adults that either lack (−, light gray bars) or express (+, dark gray bars) a rescuing-RFP::RAB-10 fusion protein from a transgene using the *glr-1* promoter. Whereas wild-type animals have small clusters of GLR-1::GFP, *rab-10* and *lin-10* mutants accumulate GLR-1 in large accretions (arrows). Cell-autonomous expression of RFP::RAB-10 rescues the *rab-10* mutant, and it can increase the number of GLR-1 clusters. Bar, 5 μm. Error bars are SEM. N = 15–20 animals for each genotype-transgene combination. *$p < 0.05$, **$p < 0.01$, ***$p < 0.001$ by analysis of variance (ANOVA) followed by Dunnett's multiple comparison to wild type.

We quantified the magnitude of the effect that various mutant backgrounds had on the localization of AMPARs by measuring the size of GLR-1::GFP fluorescent clusters. The average size of GLR-1–containing accretions in *lin-10* mutant animals was slightly larger than that observed in *rab-10* mutants (Figure 1E). However, in either mutant background, the average accretion size was nearly twice that of GLR-1 clusters found in wild-type animals. We also determined the average density (number per neurite length) of GLR-1::GFP clusters present in neurites. We found slightly fewer GLR-1–containing clusters per 10 μm in either mutant background, compared with wild-type animals (Figure 1F).

The effect of *rab-10* mutations on GLR-1 localization might be indirectly caused by general defects in synapse formation. To explore this possibility, we examined the localization of the synaptic vesicle protein synaptobrevin (SNB-1) (Nonet *et al.*, 1998). SNB-1::GFP, when expressed from the *glr-1* promoter, displays a punctate localization pattern, labeling presynaptic boutons along neurites of the command interneurons in wild-type animals (Rongo *et al.*, 1998; Shim *et al.*, 2004; Glodowski *et al.*, 2005). We observed a similar punctate localization for SNB-1::GFP in *rab-10* mutant animals (data not shown). We quantified the size and density of SNB-1::GFP puncta, and we saw little difference between wild-type and *rab-10* mutants for either of these parameters (Figure 1, E and F; dark gray bars). For SNB-1::GFP clusters, we noticed slightly decreased (but not statistically significant) puncta density in *rab-10* mutants compared with wild-type animals (Figure 1F), but the size of these puncta remained constant regardless of genetic background (Figure 1E). Mutations that are known to impair presynaptic bouton organization do not display the GLR-1 localization phenotype observed in *rab-10* and *lin-10* mutants (Rongo *et al.*, 1998; Rongo and Kaplan, 1999). Together, these findings demonstrate that the effect of *rab-10* mutations on GLR-1 trafficking is not due to gross synaptic misorganization.

To determine whether RAB-10 functions cell autonomously in neurons to regulate GLR-1, we used the *glr-1* promoter to direct expression of RFP-tagged RAB-10 (RFP::RAB-10) in *rab-10* mutant animals. We found that *rab-10* mutant animals expressing RFP::RAB-10 lacked large GLR-1::GFP–containing accretions; instead, they contained small GLR-1::GFP clusters similar to those found in wild-type animals (Figure 1, D and G). This result demonstrates that RFP::RAB-10 is functional and that RAB-10 functions in a cell-autonomous manner to direct AMPAR trafficking. To our knowledge, this is the first report of a neuronal function for RAB-10. Interestingly, upon expression of RFP::RAB-10, we observed an increase in the density of GLR-1–containing clusters in neurites of either wild-type or *rab-10* mutant animals (Figure 1H). These data suggest that RAB-10 can stimulate punctate localization of AMPARs in neuronal processes, an activity that has not been reported previously for any Rab protein.

Mutations in Either rab-10 or lin-10 Result in Behavioral Phenotypes Indicative of Decreased GLR-1 Signaling

We reasoned that the aberrant accumulation of GLR-1 observed in *rab-10* and *lin-10* mutants is likely due to defects in GLR-1 membrane trafficking. If mutations in *rab-10* or *lin-10* result in the accumulation of GLR-1 at an internal membrane trafficking compartment, then these mutations should result in corresponding GLR-1–mediated behavioral phenotypes (Burbea *et al.*, 2002; Juo and Kaplan, 2004; Shim *et al.*, 2004; Umemura *et al.*, 2005; Schaefer and Rongo, 2006). In *C. elegans*, GLR-1 signaling positively regulates spontaneous reversals during forward locomotion as animals forage for food (Mellem *et al.*, 2002; Zheng *et al.*, 2004). Backward locomotion in *C. elegans* can also be induced by stimulating the mechanosensory neuron ASH, which makes glutamatergic connections to the GLR-1–expressing interneurons

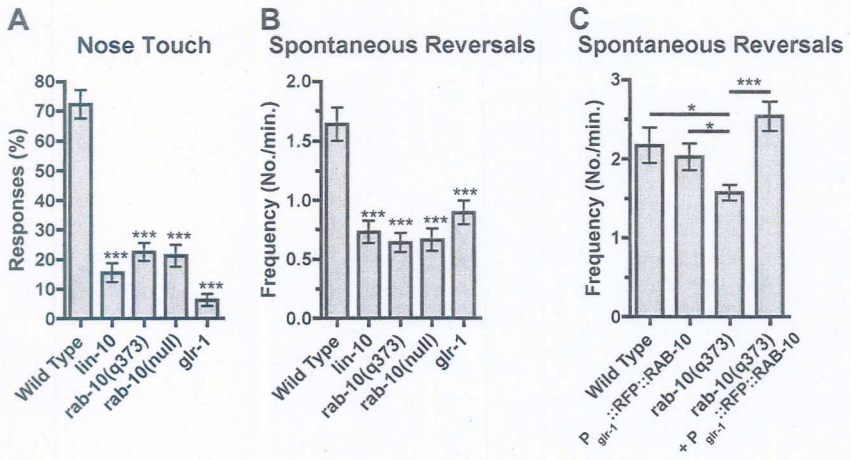

Figure 2. RAB-10 is required for GLR-1 function. (A) The mean nose-touch sensitivity (percentage of 10 total trials per animal in which the animal reversed direction upon forward collision with an eyelash) is plotted for the given genotype. (B, C) The mean spontaneous reversal frequency (number of reversals per minute over a 5-min period) is plotted for the given genotype. The animals in (C) also express GLR-1::GFP from the *nuIs25* transgene, resulting in an elevated level of reversals compared with animals that lack *nuIs25*. Error bars are SEM $*p < 0.05$, $***p < 0.001$ for comparisons to wild type using ANOVA and Dunnett's multiple comparison test. n = 15–20 animals for each genotype.

(White *et al.*, 1986; Kaplan and Horvitz, 1993). Mutants with reduced GLR-1 activity have a lower frequency of spontaneous reversals and are nose-touch insensitive, whereas mutants with increased GLR-1 activity (e.g., higher levels of synaptic GLR-1 at the cell surface) have a higher frequency of spontaneous reversals (Hart *et al.*, 1995; Maricq *et al.*, 1995; Burbea *et al.*, 2002; Mellem *et al.*, 2002; Juo and Kaplan, 2004; Shim *et al.*, 2004; Zheng *et al.*, 2004; Umemura *et al.*, 2005; Schaefer and Rongo, 2006).

We examined GLR-1–mediated behaviors in wild-type animals and in animals with mutations in *lin-10* and *rab-10*. Wild-type animals reversed direction in response to nose-touch with a frequency of ~73% (20 animals; 10 trials per animal), whereas *glr-1* mutants only reversed direction in response to nose-touch with a frequency of ~10% (Figure 2A). Like the *glr-1* mutants, both *lin-10* and *rab-10* mutants displayed significantly reduced responses to nose-touch, with frequencies near 15–20%, suggesting a reduction in GLR-1 signaling in the absence of either LIN-10 or RAB-10 protein. When spontaneous reversals were assayed, we found that wild-type animals spontaneously reversed ~1.6 times per minute (20 animals; 5-min trial per animal), whereas *glr-1* mutants only spontaneously reversed direction ~0.8 times per minute (Figure 2B). Like *glr-1* mutant animals, the *lin-10* and the *rab-10* mutants spontaneously reversed direction ~0.7 times per minute, a frequency that was statistically lower than that for wild-type animals (Figure 2B). Thus, the accumulation of GLR-1 in neurites of both *lin-10* and *rab-10* mutant animals correlates with behaviors that indicate decreased synaptic strength. We also observed rescue of behavioral defects in *rab-10* mutant animals expressing RFP::RAB-10 (Figure 2C). Interestingly, whereas expression of RFP::RAB-10 results in more GLR-1::GFP puncta, it does not result in a significant increase in reversal frequency, suggesting that the additional puncta might not be at synapses. Taken as a whole, our results demonstrate that RAB-10 and LIN-10 are required in the interneurons for GLR-1–mediated behaviors, and they suggest that RAB-10 and LIN-10 mediate the exit of GLR-1 from nonfunctional compartments within ventral cord neurites to its site of function on postsynaptic membranes.

RAB-10 and LIN-10 Function in Two Parallel Pathways to Direct GLR-1 Localization

Because we observed similar phenotypes with respect to GLR-1 localization and GLR-1–mediated behaviors in *lin-10* and *rab-10* mutant animals, we asked whether the LIN-10 and RAB-10 proteins might work together in a single pathway to mediate GLR-1 trafficking. To address this question, we examined the localization of GLR-1::GFP in *rab-10 lin-10* double mutant animals. Unexpectedly, we found a more severe defect in the accumulation of GLR-1::GFP in *rab-10 lin-10* double mutants than in either *lin-10* or *rab-10* single mutants (Figure 3A). The average size of GLR-1–containing accretions was almost twice as large in double mutants as in either single mutant (Figure 3B). In addition, we saw a slight reduction in cluster density (Figure 3C). The mean spontaneous reversal frequency of *rab-10 lin-10* double mutants was similar to that observed in *glr-1* null mutants (Figure 3D). Thus, there is an additive effect on GLR-1 localization defects caused by the presence of null mutations in *lin-10* and *rab-10*, suggesting that LIN-10 and RAB-10 proteins function in parallel pathways.

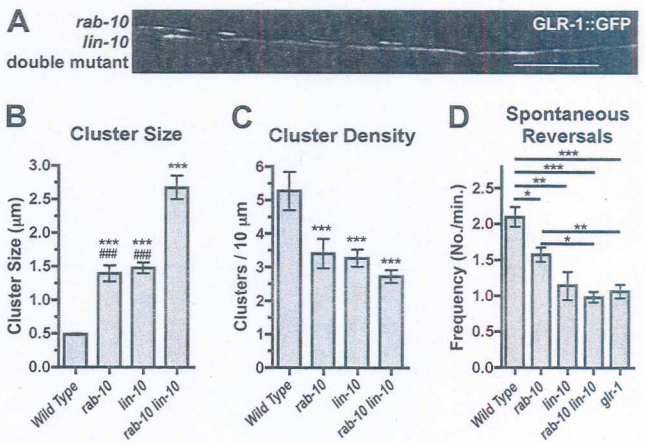

Figure 3. Parallel requirements for RAB-10 and LIN-10 in GLR-1 trafficking. (A) GLR-1::GFP fluorescence was examined in *rab-10 lin-10* double mutants. GLR-1 accumulates in accretions nearly twice the size of those in either single mutant (compare with Figure 1, A–C). The mean size (B) and density (C) of clusters are plotted for adults of the given genotype. $p < 0.001$ for comparisons to wild type (***) and *rab-10 lin-10* double mutants (###) by using ANOVA followed by Dunnett's multiple comparison test. (D) The mean spontaneous reversal frequency (number of reversals per minute over a 5-min period) is plotted for the given genotype. $*p < 0.05$, $**p < 0.01$, $***p < 0.001$ for comparisons to wild type by using ANOVA and the Bonferroni multiple comparison test for the indicated genotypes. Bar, 5 µm. n = 15–20 animals for each genotype.

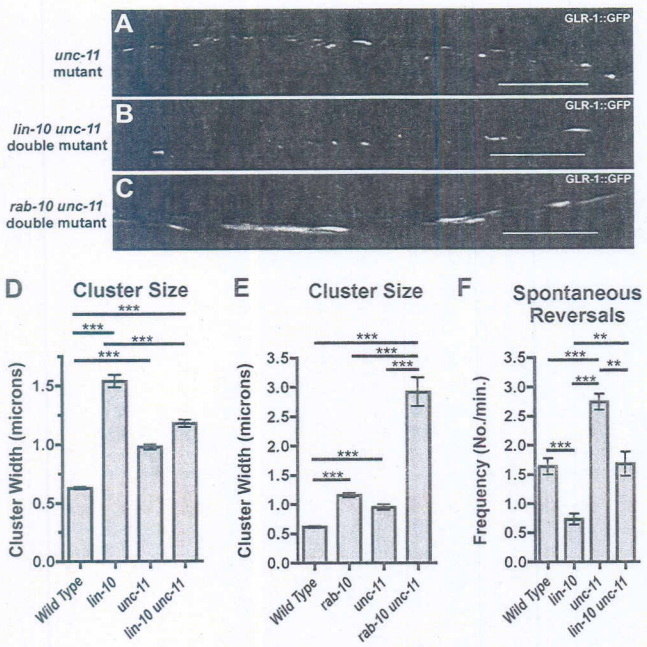

Figure 4. UNC-11 (AP180) is required for GLR-1 accumulation in *lin-10* mutants but not in *rab-10* mutants. GLR-1::GFP fluorescence was examined in *unc-11* mutants (A), *lin-10 unc-11* double mutants (B), and *rab-10 unc-11* double mutants (C). The mean size (D and E) of fluorescent clusters is plotted for adults of the given genotype. (F) The mean spontaneous reversal frequency (number of reversals per minute over a 5-min period) is plotted for the given genotype. Mutations in *unc-11* suppress the accumulation of GLR-1 in *lin-10* mutants, and they increase the accumulation of GLR-1 in *rab-10* mutants. They also completely suppress the spontaneous reversal defect in *lin-10* mutants. ***$p < 0.001$, **$p < 0.01$ by ANOVA followed by a Bonferroni multiple comparison test for the indicated comparisons. Bar, 5 μm. n = 15–20 animals for each genotype.

UNC-11 and ITSN-1 Function Upstream of LIN-10 but Not RAB-10

Based on the behavioral phenotypes of *lin-10* and *rab-10* mutants, which indicated reduced levels of GLR-1 at postsynaptic membranes, we hypothesized that the excess GLR-1 in the neurites of these animals was accumulating in an intracellular endosomal compartment. If this is true, then mutations in the endosomal machinery involved in early steps of endocytosis and trafficking should suppress the mutant phenotypes of *rab-10* and/or *lin-10*. Previously, UNC-11 (a clathrin adaptin protein AP180 orthologue that mediates endocytosis) was identified as a regulator of the synaptic abundance of AMPARs (Nonet *et al.*, 1999; Burbea *et al.*, 2002). Indeed, mutations in *unc-11* result in an ~50% increase in the size of postsynaptic GLR-1 clusters (Figure 4, A and D) (Burbea *et al.*, 2002). To determine whether either LIN-10 or RAB-10 function in a linear pathway with UNC-11, we analyzed GLR-1::GFP localization in both *lin-10 unc-11* and *rab-10 unc-11* double mutant animals. The *lin-10 unc-11* animals lacked the GLR-1–containing accretions observed in *lin-10* single mutants; instead, they contained numerous smaller clusters similar to those observed in *unc-11* mutants (Figure 4, B and D). A compelling reason for why the GLR-1 accretions found in *lin-10* mutants are diminished when clathrin-mediated endocytosis is depressed is that less GLR-1 is available to be trapped in internal compartments. By contrast, *rab-10 unc-11* animals still possessed large GLR-1-containing accretions, which were larger than those in either *unc-11* or *rab-10* single mutants (Figure 4, C and E). These results suggest that *unc-11* is epistatic to *lin-10* but not *rab-10*, consistent with the idea that LIN-10 and RAB-10 function in distinct regulatory pathways. Furthermore, the additive effect of mutations in *unc-11* and *rab-10* suggests that UNC-11 and RAB-10 function in parallel pathways. Mutations in *unc-11* also partially suppressed the decrease in spontaneous reversals observed in *lin-10* mutants (Figure 4F). Double mutants for *rab-10 unc-11* were significantly lethargic, precluding a similar behavioral analysis. Together, these data imply that the endocytosis of postsynaptic GLR-1 can occur through more than one regulated pathway and that it may be clathrin dependent (regulated by UNC-11 and LIN-10) or clathrin independent (regulated by RAB-10).

The Intersectin adaptor protein is thought to function in clathrin-dependent endocytosis by recruiting endocytosis machinery to clathrin-coated pits (Yamabhai *et al.*, 1998; Sengar *et al.*, 1999; Simpson *et al.*, 1999; Koh *et al.*, 2004; Marie *et al.*, 2004). The *C. elegans* genome contains a single Intersectin orthologue, called ITSN-1, which is most similar to *Drosophila* dynamin-associated protein of 160 kDa (Dap160) and the short isoform of human *ITSN1* (Figure 5A). ITSN-1 contains two Eps15-homology (EH) domains, an Smc/coiled coil, and five Src Homology (SH3) domains. We analyzed a deletion allele of *itsn-1*, called *ok238*, which removes the Smc/coiled coil domain and a single SH3 domain. This deletion also shifts the reading frame to preclude translation of the remaining SH3 domains. We asked whether *itsn-1(ok238)* could suppress the GLR-1 localization phenotype of *rab-10* or *lin-10* mutants by examining the localization of GLR-1::GFP in double mutant animals. We found that the average size of GLR-1-containing clusters in *itsn-1* mutant animals was only slightly larger than that in wild-type animals (Figure 5, B and E). However, a mutation in *itsn-1* suppressed the *lin-10* mutant phenotypes for GLR-1 localization (Figure 5, C and E) as well as for GLR-1–mediated behavior (Figure 5G). In addition, the *rab-10* mutant phenotype was not suppressed by an *itsn-1* mutation (Figure 5, D, E, and H). This result is consistent with our hypothesis that two parallel pathways exist for GLR-1 trafficking, regulated either by LIN-10 or RAB-10. Furthermore, these results suggest that ITSN-1 functions upstream of LIN-10 to promote GLR-1 endocytosis.

GLR-1 Accumulation in rab-10 Mutants Is Cholesterol Dependent

If GLR-1 is endocytosed by clathrin-independent endocytosis and recycled by RAB-10, then the intracellular accumulation of GLR-1 in *rab-10* mutants should be suppressed by depressing clathrin-independent endocytosis. Clathrin-independent endocytosis is highly sensitive to cholesterol levels, and it is depressed under conditions of low cholesterol (Johannes and Lamaze, 2002; Parton and Richards, 2003; Kirkham and Parton, 2005; Le Roy and Wrana, 2005). We grew wild-type, *lin-10*, and *rab-10* animals on cholesterol-depleted media for one generation, and then we examined GLR-1 localization in these animals (Merris *et al.*, 2003, 2004). Because cholesterol depletion did not affect all animals equally, we categorized GLR-1 localization for each animal as either "no phenotype" (most GLR-1 puncta are small, 0.4–0.8 μm in diameter), "medium phenotype" (animals had mostly small puncta but some larger GLR-1 puncta, 0.8–1.2 μm in diameter), or "strong phenotype" (most GLR-1 is in large accretions, usually >1.5 μm in length). Categorization was scored blindly with respect to genotype and the presence of dietary cholesterol. Cholesterol depletion of wild-type nematodes resulted in a 70% increase in the

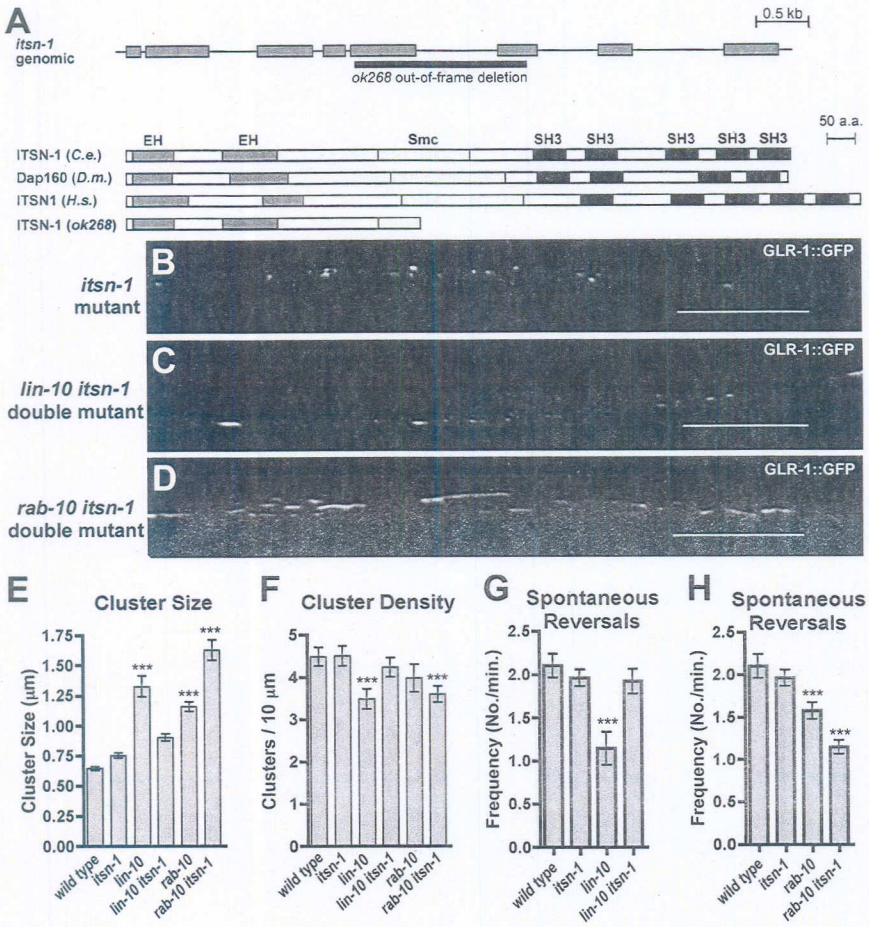

Figure 5. ITSN-1 is required for GLR-1 accumulation in *lin-10* mutants but not in *rab-10* mutants. (A) ITSN-1 encodes the sole orthologue of Intersectin 1 in *C. elegans*. The predicted intron/exon gene structure of *itsn-1* based on cDNA sequence is shown at top. Gray boxes indicate coding sequences. At bottom is the predicted protein domain structure, including EH domains, Smc/coiled-coil domain, and SH3 domains, for *C. elegans* (*C.e.*) ITSN-1, *Drosophila* (*D.m.*) Dap160, and human (*H.s.*) ITSN1. The molecular nature of the *ok268* deletion, which removes part of the Smc sequence and an SH3 domain, is shown. This deletion also shifts the reading frame, resulting in a predicted translational termination before the remaining SH3 domains; ITSN-1(ok268) indicates the predicted protein product. GLR-1::GFP fluorescence was examined in (B) *itsn-1* mutants, (C) *lin-10 itsn-1* double mutants, and (D) *rab-10 itsn-1* double mutants. The mean size (E) and the mean density (F) of fluorescent clusters are plotted for adults of the given genotype. (G and H) The mean spontaneous reversal frequency (number of reversals per minute over a 5-min period) is plotted for the given genotype. Mutations in *itsn-1* suppress the accumulation of GLR-1 in *lin-10* mutants, and they increase the accumulation of GLR-1 in *rab-10* mutants. They completely suppress the spontaneous reversal defect in *lin-10* mutants (G) but not in *rab-10* mutants (H). $p < 0.001$ for comparisons to wild type (***) by using ANOVA followed by Dunnett's multiple comparison test. Bar, 5 µm. n = 15–20 animals for each genotype.

number of animals with large puncta like those found in *unc-11* mutants (Figure 6, A, C, and F), suggesting that, like mutations in *unc-11*, cholesterol depletion can depress GLR-1 endocytosis. Cholesterol depletion of *rab-10* mutants resulted in a 40% decrease in the number of animals with large accretions. Instead, these *rab-10* mutants contained GLR-1 in mostly small clusters (Figure 6, B, D, and F), similar to those observed in wild-type animals, suggesting that cholesterol deprivation suppresses *rab-10* by preventing the internalization of GLR-1 from synaptic sites to internal compartments. Presumably, the GLR-1 accretions found in *rab-10* mutants are diminished in the absence of cholesterol, because less GLR-1 is available to be trapped in internal compartments. By contrast, cholesterol deprivation had little effect on *lin-10* mutants (Figure 6F). Our results indicate that the accumulation of GLR-1 in *rab-10* mutant neurites requires a cholesterol-dependent step.

LIN-10 and RAB-10 Are Localized to Distinct Subcellular Compartments

To determine whether RAB-10 and LIN-10 associate with similar intracellular compartments in neurons, we coexpressed LIN-10::GFP together with RFP::RAB-10, by using the *glr-1* promoter. In the intestinal epithelia of *C. elegans*, RAB-10 associates with Golgi, and it is localized mainly to early endosomes (Chen *et al.*, 2006). Previously, we showed that LIN-10 is present in Golgi and that it is localized to postsynaptic sites in neurons (Glodowski *et al.*, 2005). We found that, like LIN-10, RFP::RAB-10 is present in neuronal cell bodies as well as throughout the ventral nerve cord neurites. However, unlike LIN-10::GFP, which localizes to relatively small, uniform puncta in neurites (Figure 7A), RFP::RAB-10 localization is somewhat irregular with regard to the size and shape of clusters (Figure 7B). Generally, RFP::RAB-10-containing clusters were less abundant and larger than LIN-10::GFP-containing clusters. This could indicate that early endosomal structures in neurites are morphologically dynamic as protein trafficking rates change at different regions throughout the ventral nerve cord.

We sometimes observed close association between RFP::RAB-10 and LIN-10::GFP in neurites, as indicated by partial overlap between LIN-10::GFP and RFP::RAB-10 clusters (Figure 7C, arrowheads denote partial colocalization). We found ~20% of LIN-10::GFP puncta were associated with a cluster of RFP::RAB-10, whereas ~40% of RFP::RAB-10 clusters were associated with one or more LIN-10::GFP puncta. We also compared the localization patterns of GLR-1::GFP (Figure 7D) and RFP::RAB-10 (Figure 7F) in wild-type animals to determine whether GLR-1 clusters were colocalized with RAB-10. However, we found only ~5% of GLR-1::GFP clusters associated with RFP::RAB-10 clusters, and ~10% of RFP::RAB-10 clusters associated with GLR-1::GFP. These findings indicate that RAB-10 and LIN-10 are largely present at distinct compartments, and they raise the possibility that GLR-1 might only be transiently associated with RAB-10 in wild-type animals.

We also looked at RFP::RAB-10 and GLR-1::GFP in a *lin-10* mutant background. The localization pattern of RFP::RAB-10 was similar in wild-type (Figure 7F) and *lin-10* mutant (Figure

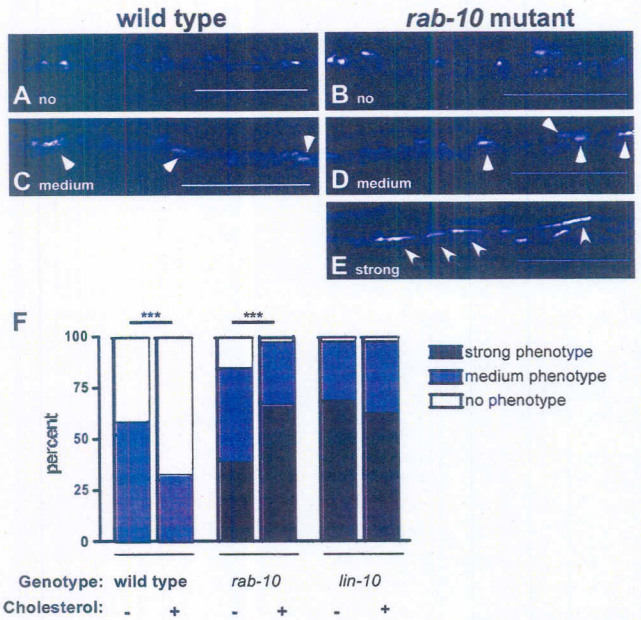

Figure 6. GLR-1 accumulation in *rab-10* mutants is cholesterol-dependent. Wild-type animals grown on cholesterol-depleted media were categorized as no phenotype (most GLR-1 puncta 0.4–0.8 μm in diameter) (A) or medium phenotype (mostly small GLR-1 puncta, with some GLR-1 puncta 0.8–1.2 μm in diameter; arrowheads) (C). Mutants for *rab-10*, when grown on cholesterol-depleted media, were similarly categorized as either no phenotype (B), medium phenotype (D), or strong phenotype (E) (contain large GLR-1 accretions >1.5 μm in length; arrows). (F) The frequency of adult animals with the indicated phenotype is plotted for each given genotype and experimental condition (plus or minus cholesterol in growth media). Animals were categorized as described above (no phenotype, white bars; medium phenotype, gray bars; or strong phenotype, black bars). Categorization was scored blindly with respect to genotype. Animals from six separate trials were examined; trial-to-trial variation was minimal. The plot contains data pooled from all six trials. n = 150–200 animals for each genotype. ***$p < 0.0001$ by Mann–Whitney *U* test.

7G) backgrounds, suggesting that LIN-10 is not required for the localization of RAB-10. In addition, we found essentially no colocalization between the GLR-1::GFP that accumulated in large accretions and RFP::RAB-10 (Figure 7I). Therefore, we conclude that GLR-1 does not accumulate in RAB-10–containing early endosomes in *lin-10* mutants. Finally, we looked at LIN-10::GFP in a *rab-10* mutant background, and we found that the localization pattern of LIN-10::GFP was similar in wild type (Figure 7J) and *rab-10* mutants (Figure 7K), suggesting that RAB-10 is not required for the localization of LIN-10.

DISCUSSION

In this study, we identified RAB-10 as a novel regulator of AMPAR trafficking. Several lines of evidence suggest that at least two distinct pathways mediate vesicular trafficking of GLR-1 near synaptic sites. First, animals with mutations in both *lin-10* and *rab-10* displayed GLR-1 localization defects that were much more severe than that of either *rab-10* or *lin-10* single mutants. Second, mutations that reduce clathrin-dependent endocytosis (e.g., *itsn-1*) suppressed the GLR-1–associated phenotypes in *lin-10* mutant animals but not those in *rab-10* mutants. Third, cholesterol depletion, which depresses clathrin-independent endocytosis mechanisms, suppressed the phenotype of *rab-10* mutants but not *lin-10* mutants. Finally, our findings showed minimal colocalization between RFP::RAB-10 and LIN-10::GFP, suggesting that RAB-10 and LIN-10 are localized to distinct subcellular compartments at steady state. However, it is possible that transient associations between RAB-10 and either GLR-1 or LIN-10 might still occur in vivo. Based on these results, we propose that RAB-10 and LIN-10 promote GLR-1 trafficking along distinct pathways by mediating exit of GLR-1 from an intracellular endosomal compartment (Figure 8).

RAB-10 has been proposed to mediate trafficking between different donor and target membranes in different cell-types. For example, in polarized Madin-Darby canine kidney (MDCK) cells, RAB-10 mediates transport from basolateral sorting endosomes to common endosomes that are accessible to both apical and basolateral recycling pathways (Babbey *et al.*, 2006). In another polarized cell type, *C. elegans* intestinal epithelia, RAB-10 is thought to mediate cargo recycling from early endosomes to recycling endosomes (Chen *et al.*, 2006). Such a hypothesis is consistent with the observation that *rab-10* mutant animals display abnormally large early endosomes and that they lack recycling endosomes in intestinal cells. Because of the relatively small size of *C. elegans* neurons compared with intestinal epithelia, it is dif-

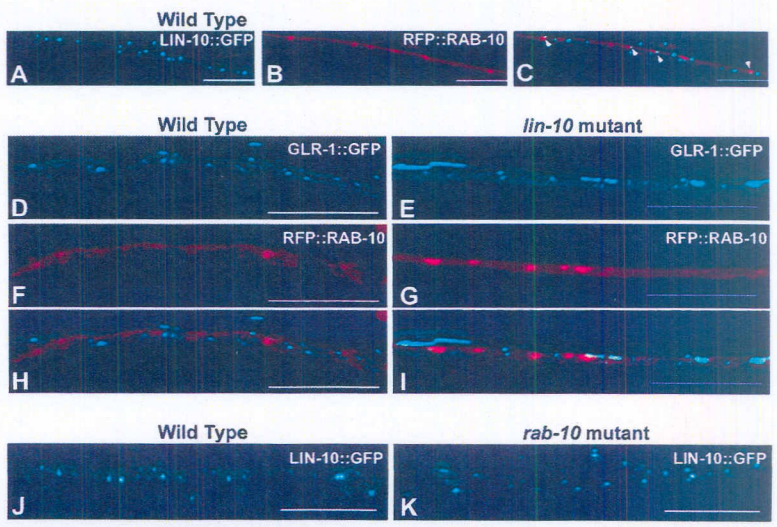

Figure 7. LIN-10 and RAB-10 are localized to distinct subcellular compartments. (A) LIN-10::GFP fluorescence. (B) RFP::RAB-10 fluorescence. (C) Merged image. Most LIN-10::GFP puncta and RFP::RAB-10 puncta are distinctly localized, although a small number are adjacent (arrows). GLR-1::GFP (D and E) and RFP::RAB-10 (F and G) fluorescence in wild-type animals (D, F, and H) or *lin-10* mutants (E, G, and I) are shown separately or in merged (H and I) images. GLR-1 accumulates in large accretions in *lin-10* mutants. Most GLR-1 in these accretions does not colocalize with RFP::RAB-10. (J and K) LIN-10::GFP fluorescence from wild-type animals (J) or *rab-10* mutants (K) are shown. LIN-10 is localized to puncta in wild type and *rab-10* mutants. Bar, 5 μm.

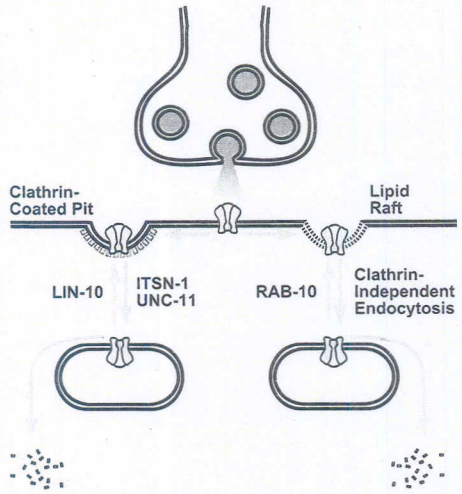

Figure 8. A model for the regulation of GLR-1 AMPAR trafficking. GLR-1 (gray channel) is endocytosed through a combination of clathrin-mediated endocytosis (indicated to left of the synapse) and clathrin-independent endocytosis (indicated to the right of the synapse). Arrows indicate major trafficking steps. In the clathrin-dependent pathway, endocytosis of GLR-1 is mediated by UNC-11 and ITSN-1. Once endocytosed, receptors can either be recycled to the synapse in a step requiring LIN-10, or degraded. By contrast, clathrin-independent endocytosis of GLR-1 requires cholesterol, and it likely proceeds through lipid rafts. Once endocytosed, receptors can either be recycled to the synapse in a step requiring RAB-10, or degraded. For either pathway, it is possible that receptors are either recycled directly to the membrane (as shown) or through additional compartments (not shown).

ficult to determine whether large vesicular structures are present in neurites of *rab-10* mutant animals. So far, our attempts to identify additional fluorescently labeled early endosomal markers with punctate localization in the nerve cord have not been successful. However, we did observe punctate localization of RFP-tagged RME-1, a marker for recycling endosomes, in the ventral nerve cord. Interestingly, this punctate localization of RFP::RME-1 persisted in both *rab-10* and *lin-10* mutant backgrounds (data not shown), suggesting that these factors are not required in neurons for the formation of RME-1–containing recycling endosomes. Moreover, GLR-1 is localized to puncta in *rme-1* mutants, similar to wild type (data not shown). Thus, in neurons, it is possible that RAB-10 and LIN-10 mediate transport from early endosomes either directly to the synaptic membrane or to a compartment other than an RME-1-containing recycling endosome. Of course, we cannot rule out that RME-1 and recycling endosomes participate in GLR-1 trafficking under specific circumstances (e.g., cellular stress, learning and memory, other forms of plasticity, et cetera).

Previously, RAB-10 was found localized within the Golgi of fibroblasts (Chen *et al.*, 1993) and sea urchin embryonic cells (Leaf and Blum, 1998), associated with common endosomes in MDCK cells (Babbey *et al.*, 2006), and within Golgi and early endosomes in *C. elegans* intestinal epithelia (Chen *et al.*, 2006). In the sensory interneurons of *C. elegans*, we found RFP::RAB-10 present in the cell bodies as well as throughout the ventral nerve cord. In the cell bodies, most of the RFP::RAB-10 accumulated in vesicular bodies that colocalized with LIN-10::GFP, which we previously showed to be associated with Golgi (Glodowski *et al.*, 2005). In the neurites of the ventral nerve cord, RFP::RAB-10–containing structures were variable in size and shape. Because the neurites of the command interneurons contain smooth membranes that resemble endosomes, but they lack clear Golgi and Golgi-resident markers, it is most likely that RFP::RAB-10 is decorating early endosomes in neurites, just as it does in epithelial cells (Rolls *et al.*, 2002). We observed low levels of colocalization between GLR-1::GFP and RFP::RAB-10, consistent with the idea that, at any one point in time, most GLR-1 in the ventral nerve cord does not reside within early endosomes. Interestingly, we saw many RFP::RAB-10 structures associated with a LIN-10::GFP puncta, raising the possibility that LIN-10 might transiently interact with RAB-10–positive endosomal compartments. However, we think that GLR-1 accumulation in *rab-10* and *lin-10* mutant animals occurs in distinct compartments, because the general morphology of RFP::RAB-10–containing clusters did not change in a *lin-10* mutant background. Similarly, the localization of LIN-10::GFP did not change in the absence of RAB-10. Early endosomes are made up of subdomains, and specific Rab GTPases delimit and occupy these subdomains; thus, it is also possible that LIN-10 and RAB-10 function at distinct subdomains on the same endosomes (Pfeffer, 2003).

Interestingly, we observed an increase in the density of GLR-1–containing clusters upon overexpression of RFP::RAB-10 in wild-type animals, suggesting that, when present in a high enough concentration, RAB-10 can stimulate the formation of GLR-1–containing puncta in neurites, perhaps by rescuing GLR-1 receptors otherwise fated for degradation. However, because we did not observe a corresponding increase in GLR-1–mediated behaviors, it is unclear whether these additional GLR-1 puncta are synaptic.

We identified *unc-11* and *itsn-1* mutants as suppressors of GLR-1–associated defects in *lin-10* but not *rab-10* mutant animals. Intersectin proteins contain multiple protein–protein interaction domains, and they have been shown to bind proteins involved in processes such as actin remodeling, signal transduction, exocytosis, and endocytosis (Roos and Kelly, 1998; Koh *et al.*, 2004; Marie *et al.*, 2004; Martin *et al.*, 2006; Evergren *et al.*, 2007). The *Drosophila* orthologue of Intersectin, Dap160, is essential for viability, and it functions as an endocytic scaffolding protein at neuromuscular junctions (Koh *et al.*, 2004; Marie *et al.*, 2004). In mammals, which have two Intersectin homologues, there is evidence suggesting that an interaction between Intersectin and the E3 ubiquitin ligase Cbl is important for endocytosis and degradation of epidermal growth factor receptor (Martin *et al.*, 2006). As in *Drosophila*, *C. elegans* has a single *itsn-1* gene, but null mutants in *C. elegans* are viable, with no obvious morphological or behavioral defects, and only subtle GLR-1 localization defects. However, we observed suppression of the *lin-10* phenotype by the *itsn-1* mutation. An *unc-11* mutation also suppressed *lin-10*, placing UNC-11 and ITSN-1 upstream of LIN-10. Both Intersectin and UNC-11/AP180 are thought to direct clathrin-mediated endocytosis (Broadie, 2004), and UNC-11 is required for the endocytosis of some ubiquitinated GLR-1 receptors (Burbea *et al.*, 2002). Why do *itsn-1* mutants not have a more dramatic GLR-1 trafficking defect by themselves? In *Drosophila*, although Dap160 mutants are lethal, absence of Dap160 results in only a mild synaptic vesicle endocytic defect compared with mutants for other components of the endocytosis machinery (Fergestad *et al.*, 1999; Verstreken *et al.*, 2002; Koh *et al.*, 2004; Marie *et al.*, 2004). Greater defects are only revealed under conditions of severe demand on the synapse (Koh *et al.*, 2004; Marie *et al.*, 2004). Thus, the contribution of ITSN-1 to GLR-1 endo-

cytosis might only be revealed in *lin-10* mutants, where the recycling of GLR-1 receptors has been impaired.

It is well accepted that endocytosis can occur by a combination of clathrin-dependent and clathrin-independent pathways, with some pathway convergence at early endosomes (Johannes and Lamaze, 2002; Kirkham and Parton, 2005). Because the accumulation of GLR-1 in *lin-10* mutants can be suppressed by blocking clathrin-dependent endocytosis (e.g., by *unc-11* and *itsn-1* mutations), LIN-10 likely recycles receptors that are endocytosed primarily by clathrin-mediated endocytosis. Indeed, mammalian orthologues of LIN-10 can interact with several small GTPases that regulate clathrin-mediated membrane trafficking (Hill *et al.*, 2003; Teber *et al.*, 2005). By contrast, the accumulation of GLR-1 in *rab-10* mutants cannot be suppressed by reducing clathrin-mediated endocytosis. Interestingly, a stronger requirement for RAB-10 is observed for the recycling of clathrin-independent cargo versus clathrin-dependent cargo in intestinal epithelia, suggesting that RAB-10 likely recycles receptors that are endocytosed primarily by clathrin-independent endocytosis (Chen *et al.*, 2006). Most forms of clathrin-independent endocytosis proceed through lipid rafts rich in cholesterol; cholesterol depletion inhibits lipid raft formation and depresses clathrin-independent endocytosis (Johannes and Lamaze, 2002; Merris *et al.*, 2003; Parton and Richards, 2003; Kirkham and Parton, 2005; Le Roy and Wrana, 2005). We find that growth on cholesterol-depleted media suppresses the accumulation of GLR-1 in *rab-10* but not *lin-10* mutants. Moreover, cholesterol depletion in wild-type animals causes GLR-1 to accumulate in a manner similar to that of blocking clathrin-dependent endocytosis (e.g., *unc-11* mutants), suggesting that interneuron synapses probably use a combination of the two endocytosis mechanisms to maintain the appropriate levels of synaptic GLR-1.

Clearly, multiple trafficking pathways are necessary to recycle GLR-1, because deficits in either LIN-10 or RAB-10 function (or in both) result in behavioral defects similar to those observed in *glr-1* null mutations. Blocking clathrin-dependent endocytosis in a *rab-10* mutant enhances the *rab-10* mutant phenotype, suggesting that GLR-1 receptors destined for clathrin-dependent endocytosis are now shunted to the clathrin-independent pathway, where they accumulate in RAB-10–containing early endosomes. Thus, the decision for a glutamate receptor to go down a given pathway seems to be made at the synapse, although this decision can be altered if one pathway is blocked. A complete understanding of how this decision is made will require the identification of the factors that specify trafficking down one pathway versus the other.

The use of both clathrin-dependent and clathrin-independent trafficking pathways to regulate the same receptor is not unprecedented. For example, the combined use of these two pathways has important consequences for the regulation of the epidermal growth factor receptor and the transforming growth factor β receptor (Le Roy and Wrana, 2005; Sigismund *et al.*, 2005). For AMPARs, multiple pathways might exist to provide neurons with more precise control over which AMPAR subunit combinations are present at a given synapse. Alternatively, the function of a particular pathway might depend on the activity of the circuit or changes in the environment. Indeed, it will be interesting to determine why a separate cholesterol-dependent AMPAR trafficking pathway exists, and what role, if any, it has in synaptic or behavioral plasticity.

ACKNOWLEDGMENTS

We thank A. Fire, the *C. elegans* Genetics Center (University of Minnesota, Minneapolis, MN), V. Maricq, J. Mendel, and R. Tsien for reagents and strains. We thank Lesley Emtage, Bonnie Firestein, EunChan Park, and Chris Trotta for comments on the manuscript. C.R. is a Pew Scholar in the Biomedical Sciences. This study was funded by National Institutes of Health grant R01 NS-42023 and the New Jersey Commission on Spinal Cord Research (to C.R.), National Institutes of Health grant R01 GM-67237 (to B.G.), and a Busch Postdoctoral Fellowship (to D.G.).

REFERENCES

Babbey, C. M., Ahktar, N., Wang, E., Chen, C. C., Grant, B. D., and Dunn, K. W. (2006). Rab10 regulates membrane transport through early endosomes of polarized Madin-Darby canine kidney cells. Mol. Biol. Cell *17*, 3156–3175.

Borg, J. P., Straight, S. W., Kaech, S. M., de Taddeo-Borg, M., Kroon, D. E., Karnak, D., Turner, R. S., Kim, S. K., and Margolis, B. (1998). Identification of an evolutionarily conserved heterotrimeric protein complex involved in protein targeting. J. Biol. Chem. *273*, 31633–31636.

Bredt, D. S., and Nicoll, R. A. (2003). AMPA receptor trafficking at excitatory synapses. Neuron *40*, 361–379.

Broadie, K. (2004). Synapse scaffolding: intersection of endocytosis and growth. Curr. Biol. *14*, R853–R855.

Brockie, P. J., Madsen, D. M., Zheng, Y., Mellem, J., and Maricq, A. V. (2001a). Differential expression of glutamate receptor subunits in the nervous system of *Caenorhabditis elegans* and their regulation by the homeodomain protein UNC-42. J. Neurosci. *21*, 1510–1522.

Brockie, P. J., Mellem, J. E., Hills, T., Madsen, D. M., and Maricq, A. V. (2001b). The *C. elegans* glutamate receptor subunit NMR-1 is required for slow NMDA-activated currents that regulate reversal frequency during locomotion. Neuron *31*, 617–630.

Brown, T. C., Tran, I. C., Backos, D. S., and Esteban, J. A. (2005). NMDA receptor-dependent activation of the small GTPase Rab5 drives the removal of synaptic AMPA receptors during hippocampal LTD. Neuron *45*, 81–94.

Burbea, M., Dreier, L., Dittman, J. S., Grunwald, M. E., and Kaplan, J. M. (2002). Ubiquitin and AP180 regulate the abundance of GLR-1 glutamate receptors at postsynaptic elements in *C. elegans*. Neuron *35*, 107–120.

Butz, S., Okamoto, M., and Sudhof, T. C. (1998). A tripartite protein complex with the potential to couple synaptic vesicle exocytosis to cell adhesion in brain. Cell *94*, 773–782.

Campbell, R. E., Tour, O., Palmer, A. E., Steinbach, P. A., Baird, G. S., Zacharias, D. A., and Tsien, R. Y. (2002). A monomeric red fluorescent protein. Proc. Natl. Acad. Sci. USA *99*, 7877–7882.

Carroll, R. C., Beattie, E. C., von Zastrow, M., and Malenka, R. C. (2001). Role of AMPA receptor endocytosis in synaptic plasticity. Nat. Rev. Neurosci. *2*, 315–324.

Carroll, R. C., Beattie, E. C., Xia, H., Luscher, C., Altschuler, Y., Nicoll, R. A., Malenka, R. C., and von Zastrow, M. (1999). Dynamin-dependent endocytosis of ionotropic glutamate receptors. Proc. Natl. Acad. Sci. USA *96*, 14112–14117.

Chen, C. C., Schweinsberg, P. J., Vashist, S., Mareiniss, D. P., and Grant, B. D. (2006). RAB-10 is required for endocytic recycling in the *C. elegans* Intestine. Mol. Biol. Cell *17*, 1286–1297.

Chen, Y. T., Holcomb, C., and Moore, H. P. (1993). Expression and localization of two low molecular weight GTP-binding proteins, Rab8 and Rab10, by epitope tag. Proc. Natl. Acad. Sci. USA *90*, 6508–6512.

Clague, M. J. (1998). Molecular aspects of the endocytic pathway. Biochem. J. *336*, 271–282.

Evergren, E., Gad, H., Walther, K., Sundborger, A., Tomilin, N., and Shupliakov, O. (2007). Intersectin is a negative regulator of dynamin recruitment to the synaptic endocytic zone in the central synapse. J. Neurosci. *27*, 379–390.

Fergestad, T., Davis, W. S., and Broadie, K. (1999). The stoned proteins regulate synaptic vesicle recycling in the presynaptic terminal. J. Neurosci. *19*, 5847–5860.

Gerges, N. Z., Brown, T. C., Correia, S. S., and Esteban, J. A. (2005). Analysis of Rab protein function in neurotransmitter receptor trafficking at hippocampal synapses. Methods Enzymol. *403*, 153–166.

Glodowski, D. R., Wright, T., Martinowich, K., Chang, H. C., Beach, D., and Rongo, C. (2005). Distinct LIN-10 domains are required for its neuronal function, its epithelial function, and its synaptic localization. Mol. Biol. Cell *16*, 1417–1426.

Hart, A. C., Sims, S., and Kaplan, J. M. (1995). Synaptic code for sensory modalities revealed by *C. elegans* GLR-1 glutamate receptor. Nature *378*, 82–84.

Hering, H., Lin, C. C., and Sheng, M. (2003). Lipid rafts in the maintenance of synapses, dendritic spines, and surface AMPA receptor stability. J. Neurosci. *23*, 3262–3271.

Hill, K., Li, Y., Bennett, M., McKay, M., Zhu, X., Shern, J., Torre, E., Lah, J. J., Levey, A. I., and Kahn, R. A. (2003). Munc18 interacting proteins: ADP-ribosylation factor-dependent coat proteins that regulate the traffic of beta-Alzheimer's precursor protein. J. Biol. Chem. *278*, 36032–36040.

Johannes, L., and Lamaze, C. (2002). Clathrin-dependent or not: is it still the question? Traffic *3*, 443–451.

Juo, P., and Kaplan, J. M. (2004). The anaphase-promoting complex regulates the abundance of GLR-1 glutamate receptors in the ventral nerve cord of *C. elegans*. Curr. Biol. *14*, 2057–2062.

Kaplan, J. M., and Horvitz, H. R. (1993). A dual mechanosensory and chemosensory neuron in *Caenorhabditis elegans*. Proc. Natl. Acad. Sci. USA *90*, 2227–2231.

Kirkham, M., and Parton, R. G. (2005). Clathrin-independent endocytosis: new insights into caveolae and non-caveolar lipid raft carriers. Biochim. Biophys. Acta *1746*, 349–363.

Koh, T. W., Verstreken, P., and Bellen, H. J. (2004). Dap160/intersectin acts as a stabilizing scaffold required for synaptic development and vesicle endocytosis. Neuron *43*, 193–205.

Le Roy, C., and Wrana, J. L. (2005). Clathrin- and non-clathrin-mediated endocytic regulation of cell signalling. Nat. Rev. Mol. Cell Biol. *6*, 112–126.

Leaf, D. S., and Blum, L. D. (1998). Analysis of rab10 localization in sea urchin embryonic cells by three-dimensional reconstruction. Exp. Cell Res. *243*, 39–49.

Malenka, R. C. (2003). Synaptic plasticity and AMPA receptor trafficking. Ann. NY Acad. Sci. *1003*, 1–11.

Malinow, R. (2003). AMPA receptor trafficking and long-term potentiation. Philos. Trans. R. Soc. Lond. B Biol. Sci. *358*, 707–714.

Man, Y. H., Lin, J. W., Ju, W. H., Ahmadian, G., Liu, L., Becker, L. E., Sheng, M., and Wang, Y. T. (2000). Regulation of AMPA receptor-mediated synaptic transmission by clathrin-dependent receptor internalization. Neuron *25*, 649–662.

Maricq, A. V., Peckol, E., Driscoll, M., and Bargmann, C. I. (1995). Mechanosensory signalling in *C. elegans* mediated by the GLR-1 glutamate receptor. Nature *378*, 78–81.

Marie, B., Sweeney, S. T., Poskanzer, K. E., Roos, J., Kelly, R. B., and Davis, G. W. (2004). Dap160/intersectin scaffolds the periactive zone to achieve high-fidelity endocytosis and normal synaptic growth. Neuron *43*, 207–219.

Martin, N. P., Mohney, R. P., Dunn, S., Das, M., Scappini, E., and O'Bryan, J. P. (2006). Intersectin regulates epidermal growth factor receptor endocytosis, ubiquitylation, and signaling. Mol. Pharmacol. *70*, 1643–1653.

Mellem, J. E., Brockie, P. J., Zheng, Y., Madsen, D. M., and Maricq, A. V. (2002). Decoding of polymodal sensory stimuli by postsynaptic glutamate receptors in *C. elegans*. Neuron *36*, 933–944.

Merris, M., Kraeft, J., Tint, G. S., and Lenard, J. (2004). Long-term effects of sterol depletion in *C. elegans*: sterol content of synchronized wild-type and mutant populations. J. Lipid Res. *45*, 2044–2051.

Merris, M., Wadsworth, W. G., Khamrai, U., Bittman, R., Chitwood, D. J., and Lenard, J. (2003). Sterol effects and sites of sterol accumulation in *Caenorhabditis elegans*: developmental requirement for 4alpha-methyl sterols. *J Lipid Res.* *44*, 172–181.

Nonet, M. L., Holgado, A. M., Brewer, F., Serpe, C. J., Norbeck, B. A., Holleran, J., Wei, L., Hartwieg, E., Jorgensen, E. M., and Alfonso, A. (1999). UNC-11, a *Caenorhabditis elegans* AP180 homologue, regulates the size and protein composition of synaptic vesicles. Mol. Biol. Cell *10*, 2343–2360.

Nonet, M. L., Saifee, O., Zhao, H., Rand, J. B., and Wei, L. (1998). Synaptic transmission deficits in *Caenorhabditis elegans* synaptobrevin mutants. J. Neurosci. *18*, 70–80.

Park, M., Penick, E. C., Edwards, J. G., Kauer, J. A., and Ehlers, M. D. (2004). Recycling endosomes supply AMPA receptors for LTP. Science *305*, 1972–1975.

Parton, R. G., and Richards, A. A. (2003). Lipid rafts and caveolae as portals for endocytosis: new insights and common mechanisms. Traffic *4*, 724–738.

Pfeffer, S. (2003). Membrane domains in the secretory and endocytic pathways. Cell *112*, 507–517.

Racz, B., Blanpied, T. A., Ehlers, M. D., and Weinberg, R. J. (2004). Lateral organization of endocytic machinery in dendritic spines. Nat. Neurosci. *7*, 917–918.

Rolls, M. M., Hall, D. H., Victor, M., Stelzer, E. H., and Rapoport, T. A. (2002). Targeting of rough endoplasmic reticulum membrane proteins and ribosomes in invertebrate neurons. Mol. Biol. Cell *13*, 1778–1791.

Rongo, C., and Kaplan, J. K. (1999). CaMKII regulates the density of central glutamatergic synapses in vivo. Nature *402*, 195–199.

Rongo, C., Whitfield, C. W., Rodal, A., Kim, S. K., and Kaplan, J. M. (1998). LIN-10 is a shared component of the polarized protein localization pathways in neurons and epithelia. Cell *94*, 751–759.

Roos, J., and Kelly, R. B. (1998). Dap160, a neural-specific Eps15 homology and multiple SH3 domain-containing protein that interacts with *Drosophila* dynamin. J. Biol. Chem. *273*, 19108–19119.

Schaefer, H., and Rongo, C. (2006). KEL-8 is a substrate receptor for CUL3-dependent ubiquitin ligase that regulates synaptic glutamate receptor turnover. Mol. Biol. Cell *17*, 1250–1260.

Sengar, A. S., Wang, W., Bishay, J., Cohen, S., and Egan, S. E. (1999). The EH and SH3 domain Ese proteins regulate endocytosis by linking to dynamin and Eps15. EMBO J. *18*, 1159–1171.

Sheng, M., and Hyoung Lee, S. (2003). AMPA receptor trafficking and synaptic plasticity: major unanswered questions. Neurosci. Res. *46*, 127–134.

Shim, J., Umemura, T., Nothstein, E., and Rongo, C. (2004). The unfolded protein response regulates glutamate receptor export from the endoplasmic reticulum. Mol. Biol. Cell *15*, 4818–4828.

Sigismund, S., Woelk, T., Puri, C., Maspero, E., Tacchetti, C., Transidico, P., Di Fiore, P. P., and Polo, S. (2005). Clathrin-independent endocytosis of ubiquitinated cargos. Proc. Natl. Acad. Sci. USA *102*, 2760–2765.

Simpson, F., Hussain, N. K., Qualmann, B., Kelly, R. B., Kay, B. K., McPherson, P. S., and Schmid, S. L. (1999). SH3-domain-containing proteins function at distinct steps in clathrin-coated vesicle formation. Nat. Cell Biol. *1*, 119–124.

Stricker, N. L., and Huganir, R. L. (2003). The PDZ domains of mLin-10 regulate its trans-Golgi network targeting and the surface expression of AMPA receptors. Neuropharmacology *45*, 837–848.

Teber, I., Nagano, F., Kremerskothen, J., Bilbilis, K., Goud, B., and Barnekow, A. (2005). Rab6 interacts with the mint3 adaptor protein. Biol. Chem. *386*, 671–677.

Umemura, T., Rapp, P., and Rongo, C. (2005). The role of regulatory interactions in UNC-43 CaMKII localization and trafficking. J. Cell Sci. *118*, 3327–3338.

Verstreken, P., Kjaerulff, O., Lloyd, T. E., Atkinson, R., Zhou, Y., Meinertzhagen, I. A., and Bellen, H. J. (2002). Endophilin mutations block clathrin-mediated endocytosis but not neurotransmitter release. Cell *109*, 101–112.

Wang, Y. T., and Linden, D. J. (2000). Expression of cerebellar long-term depression requires postsynaptic clathrin-mediated endocytosis. Neuron *25*, 635–647.

White, J. G., Southgate, E., Thomson, J. N., and Brenner, S. (1986). The structure of the nervous system of *C. elegans*. Philos. Trans. R. Soc. Lond. Biol. *314*, 1–340.

Whitfield, C. W., Benard, C., Barnes, T., Hekimi, S., and Kim, S. K. (1999). Basolateral localization of the *Caenorhabditis elegans* epidermal growth factor receptor in epithelial cells by the PDZ protein LIN-10. Mol. Biol. Cell *10*, 2087–2100.

Yamabhai, M., Hoffman, N. G., Hardison, N. L., McPherson, P. S., Castagnoli, L., Cesareni, G., and Kay, B. K. (1998). Intersectin, a novel adaptor protein with two Eps15 homology and five Src homology 3 domains. J. Biol. Chem. *273*, 31401–31407.

Zerial, M., and McBride, H. (2001). Rab proteins as membrane organizers. Nat. Rev. Mol. Cell Biol. *2*, 107–117.

Zheng, Y., Brockie, P. J., Mellem, J. E., Madsen, D. M., and Maricq, A. V. (1999). Neuronal control of locomotion in *C. elegans* is modified by a dominant mutation in the GLR-1 ionotropic glutamate receptor. Neuron *24*, 347–361.

Zheng, Y., Mellem, J. E., Brockie, P. J., Madsen, D. M., and Maricq, A. V. (2004). SOL-1 is a CUB-domain protein required for GLR-1 glutamate receptor function in *C. elegans*. Nature *427*, 451–457.